

Electrical characterization of the threshold fluence for extended defect formation in *p*-type silicon implanted with MeV Si ions

S. Fatima,^{a)} J. Wong-Leung,^{b)} J. Fitz Gerald,^{c)} and C. Jagadish^{d)}

Department of Electronic Materials Engineering, Research School of Physical Sciences and Engineering, The Australian National University, Canberra, ACT 0200, Australia

(Received 20 November 1997; accepted for publication 7 April 1998)

Preamorphous damage in *p*-type Si implanted with MeV Si ions and annealed at elevated temperature is characterized using deep level transient spectroscopy (DLTS) and transmission electron microscopy (TEM). *P*-type Si was implanted with 4 MeV Si at doses from 1×10^{13} to 1×10^{14} cm⁻² and annealed at 800 °C for 15 min. For doses below this critical dose, a sharp peak is observed in the DLTS spectrum, corresponding to the signature of point defects. Above the critical dose, a broad DLTS peak is obtained, indicating the presence of extended defects. This behavior is found to be consistent with TEM analyses where extended defects are only observed for doses above the critical dose. This suggests a critical dose at which point defects from implantation act as nucleating sites for extended defect formation. © 1998 American Institute of Physics. [S0003-6951(98)03423-8]

Controlling defects is a major task for the semiconductor industry. The need for submicron device lengths for shallow junction regimes demands a detailed understanding of defect evolution and defect-defect interactions during thermal processing of Si. Postimplant annealing is known to produce extended defects above threshold doses and transient enhanced diffusion (TED) of dopants.¹⁻⁵

Ion implantation creates point defects (vacancies and interstitials) due to nuclear collisions of incoming ions with the Si lattice. Most point defects recombine during annealing and the resulting damage is mainly interstitial defects. The excess interstitials leading to extended defects are related to the implanted dose as postulated by the so called +1 model with each implanted ion contributing to roughly one excess interstitial.^{7,8} Recent experiments^{9,10} have focused on point defects and their annealing kinetics for a better understanding of the factors which influence the evolution of implant damage in both low and high dose regimes. Despite several years of research, the knowledge is still limited and the basic question as to how point defects cluster and generate extended defects is far from resolved.

In this letter, we establish a correlation between electrically active defects in ion implanted and annealed *p*-type Si, characterized by capacitance-voltage (*C-V*) measurements and deep level transient spectroscopy (DLTS), and structural defects imaged by transmission electron microscopy (TEM). The implantation doses used in this study were insufficient to form an amorphous layer and hence called preamorphous damage. DLTS was used to identify a transition dose from point to extended defects using a range of implant doses. DLTS determines the concentration of the deep levels and their signatures (activation energy and capture cross section).

It is well known that the DLTS peaks are sharp and follow exponential capture kinetics for point defects whereas broad features with logarithmic capture kinetics are reported for extended defects.¹¹ TEM examination was used to characterize extended defect microstructures and confirm the DLTS results. Such a DLTS and TEM correlation has already been reported in *n*-type Si implanted with Si, Ge, and Sn and annealed at 900 °C, where a critical dose has been established below which no electrically active defects are observed and above which extended defects are seen.¹² In this letter we report, for the first time, on the correlation between DLTS and TEM results for preamorphous damage in *p*-type Si.

Czochralski (CZ) *p*-type Si (100) boron doped with a resistivity of 6–8 Ω cm was implanted with 4 MeV Si ions at room temperature. The projected range of the ions was around 2.89 μm. Irradiation was carried out using the NEC 1.7 MV Tandem accelerator at the Australian National University. The Si substrate was tilted 7° off axis with respect to the incoming ions to reduce channeling. After implantation, the samples were annealed at 800 °C for 15 min in a conventional quartz furnace under an Ar ambient. The samples were then chemically cleaned, including a final dip in diluted HF to remove any surface oxide. Immediately after cleaning, Schottky barrier diodes were fabricated by evaporation of Ti onto the samples. *C-V* and DLTS measurements were performed as described in Ref. 13. Eight DLTS spectra with rate windows between (100 ms)⁻¹ and (12 800 ms)⁻¹ were simultaneously recorded during one single temperature scan from 77 to 300 K. A lock-in type weighting function was applied to extract the DLTS signal from the transients recorded. *C-V* measurements were used to monitor changes in background doping resulting from the formation of donors or inactive dopant complexes. A neutral defect complex involving a dopant atom is also considered to be an electrically active defect. Cross-sectional transmission electron microscopy samples were prepared using mechanical polishing, dimpling and ion beam thinning. TEM was carried out on

^{a)}Electronic-mail: shff09@rsphysse.anu.edu.au

^{b)}Also at: Australian Key Centre for Microscopy and Microanalysis, University of Sydney, NSW 2006, Australia.

^{c)}Research School of Earth Sciences, The Australian National University, Canberra, ACT 0200, Australia.

^{d)}Electronic-mail: cxj109@rsphysse.anu.edu.au

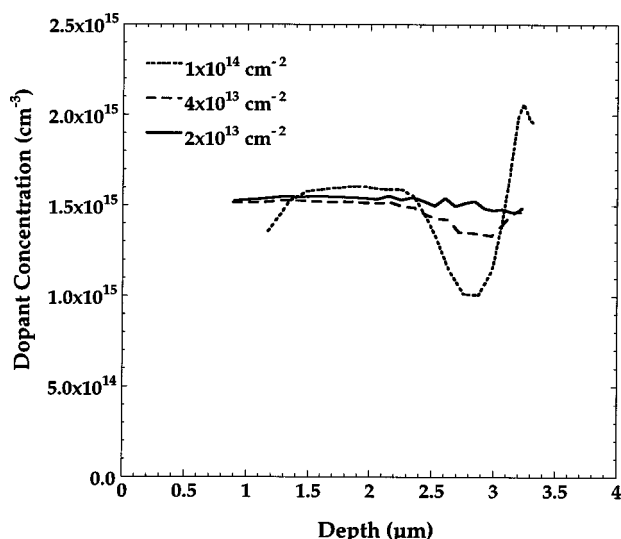


FIG. 1. Doping concentration vs depth extracted from the C - V measurements at room temperature after Si implantation and annealing.

selected samples to identify and characterize defects using a Philips 430 instrument.

Figure 1 shows the C - V profiles for various Si implanted samples after annealing. The formation of donors or inactive dopant complexes can result in changes in the background doping and can be monitored by C - V measurements. For a dose of $2 \times 10^{13} \text{ cm}^{-2}$, a constant doping profile identical to that for the unimplanted material is observed. This does not rule out the presence of point defects. For the higher doses of 4×10^{13} and $1 \times 10^{14} \text{ cm}^{-2}$, C - V measurements show a nonconstant doping profile, indicating the presence of electrically active defects with maximum concentration at a depth of $\sim 2.8 \mu\text{m}$. This compensation depth coincides well with the projected ion range of $2.8 \mu\text{m}$ obtained from TRIM 95.¹⁴ However, the sensitivity of the C - V is limited to 10% of the background doping. In contrast, the high sensitivity of DLTS for the detection of electrically active defects ($\geq 10^{11} \text{ cm}^{-3}$), allows this method to be used for samples with and without dopant compensation.

DLTS spectra corresponding to the three doses in Fig. 1 are shown in Fig. 2. For $2 \times 10^{13} \text{ cm}^{-2}$, the DLTS spectrum shows a sharp peak, having an activation energy of $E_v + (0.28 \pm 0.01) \text{ eV}$, with a capture cross section of $2.7 \times 10^{-16} \text{ cm}^2$. Increasing the ion fluence to $4 \times 10^{13} \text{ cm}^{-2}$ results in broad features appearing on the low and high temperature shoulders of this peak. From the DLTS spectra, it is evident that for the dose of $4 \times 10^{13} \text{ cm}^{-2}$, the amplitude of the defect level $E_v + (0.28 \pm 0.01) \text{ eV}$ is significantly lower than that for the $2 \times 10^{13} \text{ cm}^{-2}$ dose. With a further increase in the dose to $1 \times 10^{14} \text{ cm}^{-2}$, the amplitude of the broad features, as well as $E_v + (0.28 \pm 0.01) \text{ eV}$, appears to increase. However, in samples with carrier compensation (the two highest doses), DLTS measurements give only qualitative information. We note that in all cases, the peak at $E_v + (0.28 \pm 0.01) \text{ eV}$ was sharp and characteristic of point defects.¹¹ Indeed, the hole capture kinetics of this level showed an exponential dependence on filling pulse width, hence not supporting the formation of electrically active point defect clusters or extended defects. In addition to the level at $E_v + (0.28 \pm 0.01) \text{ eV}$, an additional level at

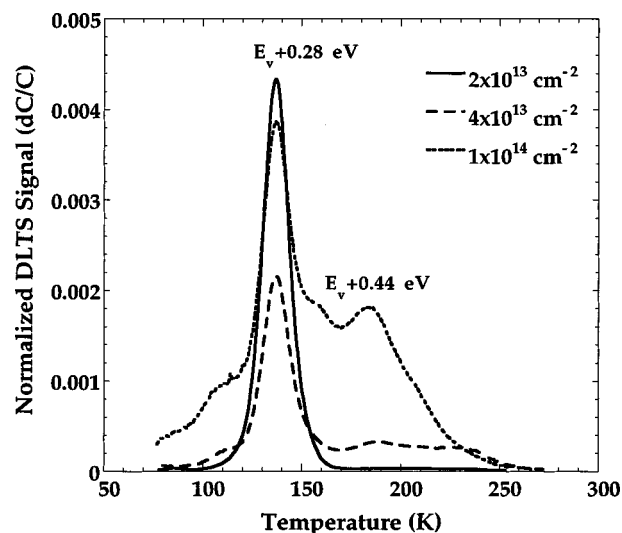


FIG. 2. DLTS spectra [window $(3200 \text{ ms})^{-1}$] of various doses below and above the transition from point defects to extended defects after 4 MeV Si ion implantation and thermal annealing at 800°C , 15 min. Bias voltage -12 V , pulse amplitude 11.5 V , pulse width 50 ms .

$E_v + (0.44 \pm 0.01) \text{ eV}$ merges for higher doses, with a capture cross section of $9.5 \times 10^{-15} \text{ cm}^2$. Interestingly, this level is seen only for doses $\geq 4 \times 10^{13} \text{ cm}^{-2}$.

The various samples described above were analyzed by TEM to examine the microstructure of the samples. The sample with an implant dose of $2 \times 10^{13} \text{ cm}^{-2}$ showed no extended defect formation throughout the sample within the detection limit of $\sim 10^{12} \text{ cm}^{-3}$. This is consistent with the DLTS spectra which showed the presence of point defects only. TEM examination of the samples subject to the higher dose implants, namely 4×10^{13} and $1 \times 10^{14} \text{ cm}^{-2}$, showed the formation of rodlike $\{311\}$ defects. This suggests a critical transition dose at which point defects are transformed into extended defects. Figures 3(a) and 3(b) are typical TEM micrographs of the samples implanted with Si to a dose of 4×10^{13} and $1 \times 10^{14} \text{ cm}^{-2}$, respectively, and annealed at 800°C for 15 min. These micrographs clearly indicate that, as expected, an increasing implant dose results in a higher density of rodlike $\{311\}$ defects. The $\{311\}$ defects are planar defects with a line orientation of $\langle 011 \rangle$ and with a dilation perpendicular to the habit plane.¹⁵ These defects have been characterized as Si interstitial agglomerations and have been shown to be a major source of TED of boron in Si.¹⁶ The TEM results are consistent with the interpretation that the broad features in the DLTS spectra correspond to the presence of extended defects.

Our results show that a critical dose exists for extended defect formation after annealing at 800°C for 15 min. This dose characterizes a transformation from point to extended defects. Below this critical dose, point defects are observed and their origin needs to be identified. In n -type Si, vacancy type defects are observed in DLTS studies¹⁷⁻¹⁹ whereas, in p -type Si, both vacancy and interstitial-type defects²⁰ have been observed. Our earlier studies in n -type Si²¹ at low ion doses ($\leq 10^{10} \text{ cm}^{-2}$) in the dilute concentration regime have shown that vacancy-type defects annihilate above about 400°C . Thus although the doses are higher by >200 times, it is significant that, in the present study, point defects are present in p -type Si even after high temperature annealing at

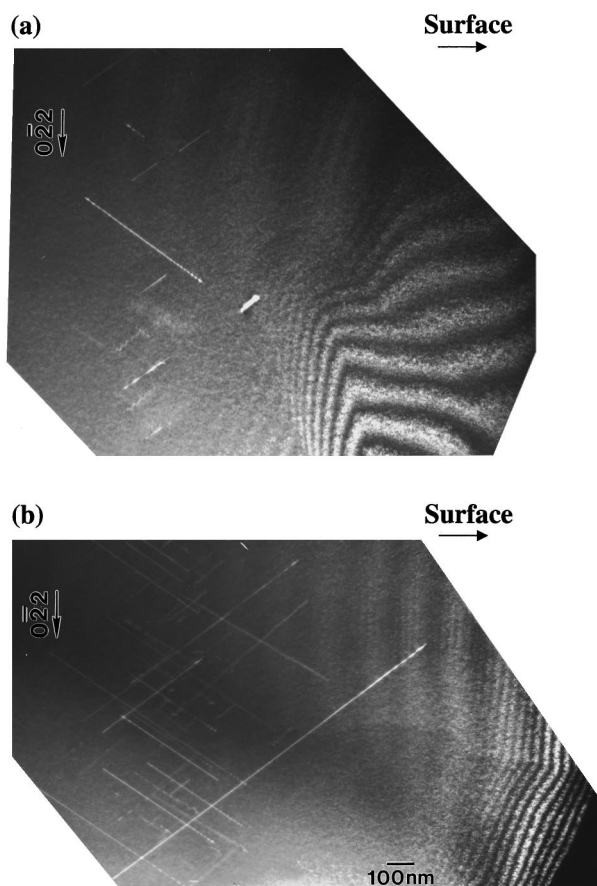


FIG. 3. Weak-beam micrographs showing the presence of the $\{311\}$ defects for (a) $4 \times 10^{13} \text{ cm}^{-2}$ and (b) $1 \times 10^{14} \text{ cm}^{-2}$.

800 °C for 15 min. However, Benton *et al.*¹⁰ have reported point defect clusters, suggested to be interstitial-based for similar doses to ours, but for annealing at 680 °C. It is likely that such clusters break up at 800 °C and release point defects, which presumably involve excess interstitials. This suggests that the point defects observed in our case most likely involve interstitials, but the exact nature of these defects is unknown at this stage.

Above the critical dose, $\{311\}$ defects were observed in the present study after annealing at 800 °C for 15 min. Jones *et al.*⁵ have suggested that it is the number of atoms introduced into the Si lattice that determines whether or not extended defects will ultimately form. During high temperature annealing, vacancies and interstitials created during implantation recombine, leaving excess interstitials in proportion to the implanted dose (the +1 model). Below a certain critical value, these excess interstitials do not form into extended defects as critical dimensions for their stable growth are not achieved. For doses above the critical value, $\{311\}$ defects nucleate. Alternatively, Schreutelkamp *et al.*²² have suggested that secondary defects, such as $\{311\}$ defects and loops, will only form after elevated temperature annealing if the number of Si atoms displaced during implantation exceeds a critical value, the so-called atomic displacement model. The nature of as-implanted defects produced by self-ion implantation of Si has been shown to be a sensitive function of implantation temperature by Elliman and Mitchell.²³ However, the concentration of extended defects formed by subsequent high temperature annealing was shown to be in-

sensitive to such variations and still depends on parameters which scale with the ion fluence. In the present case of Si implanted *p*-Si, a critical dose required to form extended defects after high temperature annealing is also consistent with the atomic displacement model²⁰ for residual defect formation. Thus, the present results do not distinguish between the +1 and atomic displacement models for residual defect formation.

In summary, in the preamorphous damage regime using MeV Si ion implantation in *p*-type Si and annealing at elevated temperature, a critical dose is established below which only point defects are present and above which $\{311\}$ defects are observed. DLTS observations correlate well with the TEM analyses: samples with only narrow point defect signatures in the DLTS spectra show no defects in TEM, while samples showing broad features in the DLTS spectra show the formation of rodlike $\{311\}$ defects in TEM.

S.F. acknowledges financial support from AusAID. Discussions with J. S. Williams, C. T. Chou, Zou Jin, D. J. H. Cockayne, B. G. Svensson, R. G. Elliman, and P. Kringhøj are acknowledged. Aleksei Boiko is acknowledged for assistance in preparing the Schottky-barrier structures.

- ¹P. A. Stolk, H. J. Gossmann, D. J. Eaglesham, D. C. Jacobson, J. M. Poate, and H. S. Luftman, *Appl. Phys. Lett.* **66**, 568 (1995).
- ²H. J. Gossmann, C. S. Rafferty, H. S. Luftman, F. C. Unterwald, T. Boone, and J. M. Poate, *Appl. Phys. Lett.* **63**, 639 (1993).
- ³N. E. B. Cowern, K. T. F. Janssen, and H. F. F. Joss, *J. Appl. Phys.* **68**, 6191 (1990).
- ⁴M. Tamura, N. Natsuaki, Y. Wada, and E. Mitani, *Nucl. Instrum. Methods Phys. Res. B* **21**, 438 (1987).
- ⁵K. S. Jones, S. Prussin, and E. R. Weber, *Appl. Phys. A: Solids Surf.* **45**, 1 (1988).
- ⁶M. Jaraiz, G. H. Gilmer, J. M. Poate, and T. D. de la Rubia, *Appl. Phys. Lett.* **68**, 409 (1996).
- ⁷M. D. Giles, *J. Electrochem. Soc.* **138**, 1160 (1991).
- ⁸D. J. Eaglesham, P. A. Stolk, H.-J. Gossmann, T. E. Haynes, and J. M. Poate, *Nucl. Instrum. Methods Phys. Res. B* **106**, 191 (1995).
- ⁹S. Libertino, J. L. Benton, D. C. Jacobson, D. J. Eaglesham, J. M. Poate, S. Coffa, P. G. Fuochi, and M. Lavallo, *Appl. Phys. Lett.* **70**, 3002 (1997).
- ¹⁰J. L. Benton, S. Libertino, P. Kringhøj, D. J. Eaglesham, J. M. Poate, and S. Coffa, *J. Appl. Phys.* **82**, 120 (1997).
- ¹¹P. Omeling, E. R. Weber, L. Montelius, H. Alexander, and J. Michel, *Phys. Rev. B* **32**, 6571 (1985).
- ¹²P. Kringhøj, J. S. Williams, and C. Jagadish, *Appl. Phys. Lett.* **65**, 17 (1994).
- ¹³J. Lalita, Ph. D. thesis, Royal Institute of Technology, Sweden, 1997 (unpublished).
- ¹⁴J. P. Biersack and L. G. Haggmark, *Nucl. Instrum. Methods* **174**, 257 (1980).
- ¹⁵C. A. Ferreira Lima and A. Howie, *Philos. Mag.* **34**, 1057 (1976).
- ¹⁶D. J. Eaglesham, P. A. Stolk, H. J. Gossmann, and J. M. Poate, *Appl. Phys. Lett.* **65**, 2305 (1994).
- ¹⁷B. G. Svensson, C. Jagadish, and J. S. Williams, *Phys. Rev. Lett.* **71**, 1860 (1993).
- ¹⁸B. G. Svensson, C. Jagadish, and J. S. Williams, *Nucl. Instrum. Methods Phys. Res. B* **80/81**, 583 (1993).
- ¹⁹B. G. Svensson, C. Jagadish, A. Hallen, and J. Lalita, *Phys. Rev. B* **55**, 10 498 (1997).
- ²⁰J. Lalita, N. Kesitalo, A. Hallen, C. Jagadish, and B. G. Svensson, *Nucl. Instrum. Methods Phys. Res. B* **120**, 27 (1996).
- ²¹J. Lalita, B. G. Svensson, C. Jagadish, and A. Hallen, *Nucl. Instrum. Methods Phys. Res. B* **127/128**, 69 (1997).
- ²²R. J. Schreutelkamp, J. S. Custer, J. R. Liefting, W. X. Lu, and F. W. Saris, *Mater. Sci. Rep.* **6**, 275 (1991).
- ²³R. G. Elliman and I. V. Mitchell, *Mater. Res. Soc. Symp. Proc.* **273**, 469 (1995).